RSC Advances

PAPER

View Article Online
View Journal | View Issue

Cite this: *RSC Adv.*, 2018, **8**, 29385

Acetylcholinesterase-functionalized two-dimensional photonic crystals for the detection of organophosphates†

Fenglian Qi,[a] Yunhe Lan,[a] Zihui Meng,*[a] Chunxiao Yan,[b] Shuguang Li,[b] Min Xue,[a] Yifei Wang,[a] Lili Qiu,[a] Xuan He[c] and Xueyong Liu[c]

Received 10th June 2018
Accepted 5th August 2018

DOI: 10.1039/c8ra04953j

rsc.li/rsc-advances

Due to the indiscriminate usage of organophosphates in military and agriculture, there is an increasing demand to develop sensors for monitoring organophosphorus nerve agents and pesticides. Herein, a sensitive two-dimensional photonic crystal (2D-PC) biosensor as a part of a portable device for the detection of Dipterex is presented. The 2D-PC array was self-organized on the water–air interface using 600 nm polystyrene (PS) colloidal particles, and it was further embedded into a polyacrylamide-acrylic acid (PAM-AA) hydrogel. After condensation between the amine groups of acetylcholinesterase (AChE) and the carboxyl groups of the hydrogel, a novel sensing platform of 2D-PC hydrogel with AChE as the recognition agent was constructed. The lattice spacing of AChE-functionalized 2D-PC was inversely proportional to the logarithm of the Dipterex concentration from 10^{-14} mol L^{-1} to 10^{-4} mol L^{-1} with estimated limit of detection (LOD) of 7.7×10^{-15} mol L^{-1}. Simultaneously, the structural color of AChE-functionalized 2D-PC varied from yellow to blue. The biosensor achieved "naked-eye" detection due to which the use of AChE-functionalized 2D-PC is a promising technique for onsite and fast screening of organophosphates.

Introduction

Dipterex ($C_4H_8Cl_3O_4P$) (Fig. 1) is extensively employed in agriculture due to its ability to inhibit cholinesterase in organisms, and it can further produce more toxic dichlorvos under alkaline conditions and kill insects with high efficiency. However, generally, Dipterex is also known as a target for chemical sensors as it can mimic a nerve agent, and the remaining Dipterex on crops also contaminates the environment and is harmful to human health. Therefore, intensive attention is focused on the determination of Dipterex and other organophosphates with efficient methods, such as fluorescent sensors,[1,2] chromogenic recognition,[3] quartz-crystal-microbalance (QCM)[4,5] and surface enhanced Raman spectroscopy (SERS).[6,7] However, a potential drawback of the above methods is the requirement of instruments with high cost and large sample volumes during the monitoring of target analytes, which can cause inconvenience in the field detection. Thus, designing a portable chemical sensor with a simple and rapid protocol for the determination of organophosphates is of great importance in the areas of public safety and environmental protection.

To overcome such drawbacks, photonic crystals (PCs) have attracted considerable interests as chemical sensors because of their portability, tunable structural color and simple detection device. As a typical sensor for the determination of organophosphates, Seo *et al.* proposed core–shell colloidal crystal arrays (CCA) for the detection of paraoxon with LOD of 0.024 ppm.[8,9] They also designed a β-cyclodextrin-modified polymerized crystalline colloidal array (PCCA) thin film to detect paraoxon-ethyl and parathion-ethyl with a quick

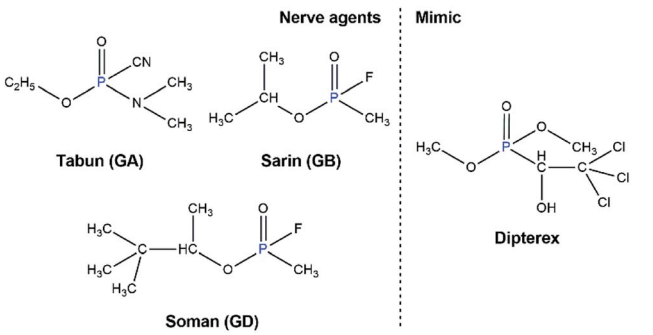

Fig. 1 Organophosphorus nerve agents and their mimic, Dipterex.

[a]School of Chemistry and Chemical Engineering, Beijing Institute of Technology, Beijing, 100081, China. E-mail: m_zihui@yahoo.com; Fax: +86 10 68913065; Tel: +86 10 68913065

[b]Institute of NBC Defence, Beijing, 102205, China

[c]Institute of Chemical Materials, China Academy of Engineering Physics, Mianyang, 621900, China

† Electronic supplementary information (ESI) available. See DOI: 10.1039/c8ra04953j

response time (10 s) and high sensitivity with LODs of 2.0 and 3.4 ppb, respectively.[10] Besides, we have previously demonstrated a molecularly imprinted photonic crystal (MIPC) to monitor the degradation product methyl phosphonic acid of the nerve agents including Sarin, Soman, VX and R-VX, with the corresponding LODs of 3.5×10^{-6} mol L^{-1}, 2.5×10^{-5} mol L^{-1}, 7.5×10^{-5} mol L^{-1} and 7.5×10^{-5} mol L^{-1},[11] which can also provide an indirect method to detect organophosphorus nerve agents.

So far, enzyme techniques have been predominantly introduced with respect to organophosphate-detecting sensors as enzymes provide active sites, which can enable reversible or irreversible combination with analytes to substantially improve selectivity. Various enzyme-based sensors, such as amperometric biosensors,[12–15] quantum dots,[16,17] silver nanoparticles[18–21] and silicon materials,[22,23] have been widely used in the area of organophosphate detection. However, these sensors also have the disadvantage of relying on specific instruments that are difficult to be applied for on-site detection. With the combination of PC and the enzyme technique, the sensor can not only realize the selectivity to organophosphates, but also have the potential to achieve semi-quantitative detection by the naked eye. In this area, Asher *et al.* prepared 3D-PCs immobilized with AChE[24] and organophosphorus hydrolase (OPH)[25] for the detection of parathion and methyl paraoxon with LODs of 4.26×10^{-12} mol L^{-1} and 2.0×10^{-7} mol L^{-1}, respectively. Hirsch *et al.* developed AChE-functionalized 3D-PC for the detection of acetylcholine from 1×10^{-9} mol L^{-1} to 1×10^{-5} mol L^{-1} and the AChE inhibitor neostigmine at LOD of 1×10^{-12} mol L^{-1}.[26] Butyrylcholinesterase (BuChE)-based 3D-PC was also prepared for the detection of sarin with LOD as low as 1×10^{-15} mol L^{-1}.[27] However, some shortcomings of 3D-PC, such as time-consuming preparation and slow mass transfer ability, limit its applications as a simple and rapid chemical sensor. Consequently, on the basis of these studies, the integration of AChE and 2D-PC, also named as the monolayer PC, was taken into account for the detection of organophosphates. Compared to 3D-PC, 2D-PC could not only realize the self-assembly preparation in just several minutes, but could also form a Debye diffraction ring under the illumination of a commercial laser pointer, which can be easily applied to quantify the variation of analyte concentration.[28,29] However, until now, only a few studies have been reported about the detection of organophosphates *via* 2D-PC.

In this research, we developed a 2D-PC biosensor based on AChE as the molecular recognition agent for the naked-eye detection of the nerve agent stimulant Dipterex. This biosensor could realize the determination of Dipterex from 10^{-14} mol L^{-1} to 10^{-4} mol L^{-1}. With the increasing concentration of Dipterex, the lattice spacing of AChE-functionalized 2D-PC decreased, which finally induced a blue-shift in the structural color and a decrease in the diameter of the Debye diffraction ring. Thus, we developed an easy and general method for the colorimetric detection of organophosphates such as nerve agents and organophosphorus pesticides.

Experimental section

Materials

Styrene, L-cysteine hydrochloride, 2-hydroxyethyl methacrylate (HEMA), *N*,*N*′-methylenebisacrylamide (BIS) and diethoxyacetophenone (DEAP) were purchased from J&K Scientific Ltd. (China). 1-Propanol, sodium dodecyl sulfate (SDS), 5,5′-dithiobis(2-nitrobenzoic acid) (DTNB), acetylthiocholine iodide (ATChI), Coomassie Brilliant Blue (G-250), dichlorvos, malathion, methidathion, acephate, glufosinate-ammonium, and Dipterex were purchased from Aladdin Co., Ltd. (China). Acrylic acid (AA) was purchased from Tokyo Chemical Industry Co., Ltd. (Japan). H_2SO_4 (95–98 wt%), phosphoric acid, HCl, NaOH, $K_2S_2O_8$ and dimethyl sulfoxide (DMSO) were purchased from Beijing Chemical Plants (China). Tris(hydroxymethyl) aminomethane (Tris) and acetylcholinesterase (AChE) were obtained from Sigma (USA). Acrylamide (AM) was purchased from Amresco (USA). H_2O_2 (30 wt%) was purchased from Tianjin Fuyu Fine Chemical Co., Ltd. (China). 1-(3-Dimethylaminopropyl)-3-ethylcarbodiimide hydrochloride (EDC) was supplied by Shanghai Medpep Co., Ltd. (China). The inhibitor in styrene needed to be removed through an Al_2O_3 column before use, whereas the other materials were used as received. Deionized water was produced by the Puris-Evo CB Water System.

Fabrication of AChE-functionalized 2D-PC

The fabrication of AChE-functionalized 2D-PC and its response to the analytes are illustrated in Fig. 2. Monodispersed PS colloidal particles (600 nm) were prepared following

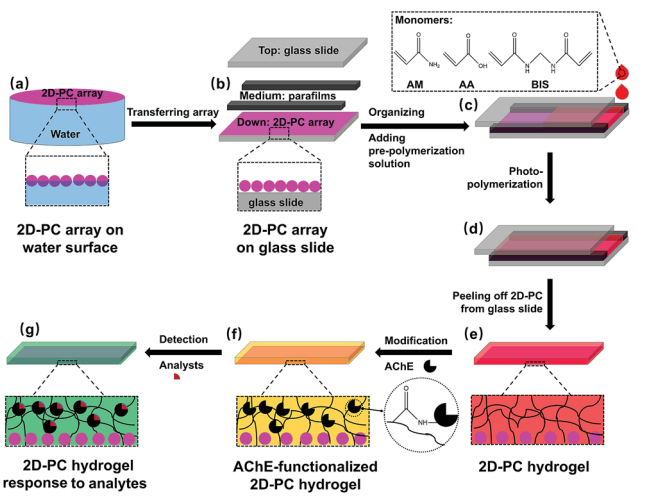

Fig. 2 Fabrication of AChE-functionalized 2D-PC and its response to analytes, (a) monodispersed PS spheres self-assembled into a 2D-PC array at the water/air interface, (b) the 2D-PC array was transferred onto a glass slide and then organized into a 'sandwich' structure with parafilm as the spacer, (c) the pre-polymerization solution was added into the 'sandwich' type, (d) photo-polymerization of the 2D-PC hydrogel, (e) the 2D-PC hydrogel was peeled off from the glass slide, (f) AChE was immobilized on the 2D-PC hydrogel, (g) the process of 2D-PC hydrogel responding to Dipterex.

a previously reported method.[30] Briefly, 205 mL of deionized water, 77.3 mL (70 g) of styrene and 1.86 mL (2 g) of HEMA were mixed thoroughly under 350 rpm and bubbled with nitrogen for 1 hour. After the temperature was increased to 70 °C, 0.11 g of $K_2S_2O_8$ dissolved in 5 mL of water was added. The resulting mixture was refluxed for 24 hours under nitrogen. After separation by centrifugation and washing with water for several times, the PS particles were adjusted to 20 wt% for further usage.

For the fabrication of a periodic 2D-PC array with a close-packed monolayer (Fig. 2a), 1-propanol and the PS suspension (20 wt%) were first mixed thoroughly at a volume ratio of 1 : 1. The resulting mixture was loaded into a syringe and then slowly spread over the water/air interface to obtain a 2D-PC array, which was finally transferred to a hydrophilic glass slide (25.4 mm × 76.2 mm × 1 mm). The glass slide needed to be pre-treated by H_2SO_4/H_2O_2 (7/3, v/v) solution overnight before use.

After the 2D-PC array was dried in air, a parafilm with a thickness of 125 μm was attached onto the 2D-PC array-loaded glass slide as a spacer; then, another glass slide was placed covering it to form a 'sandwich' (Fig. 2b). Also, 0.36 g (5.04 mmol) of AM, 38.5 mL (0.56 mmol) of AA, 10 mg (0.065 mmol) of BIS, 10 wt% DEAP (13.6 μmol, in DMSO) and 2 mL of water were mixed thoroughly and bubbled with nitrogen for 10 min to form a pre-polymerization solution. After 150 μL of the pre-polymerization solution was injected (Fig. 2c and d), the 'sandwich' structure was photo-polymerized under UV light at 365 nm for 2 hours at 5 °C. The resulting PAM-AA 2D-PC hydrogel was peeled off from the glass slide and immersed in water overnight (Fig. 2e).

For the immobilization of AChE on 2D-PC hydrogel, 3.9 mg (2000 U) of AChE was diluted into 4 mL of Tris–HCl buffer (0.15 mol L^{-1}, pH = 7.4, adjusted by HCl). Twelve pieces of the 2D-PC hydrogel (each piece was 0.5 × 0.5 cm) were first incubated in 4 mL of the AChE solution for 48 hours before being immersed in 8.35 × 10^{-5} mol L^{-1} EDC solution for 2 hours. Subsequently, the 2D-PC hydrogels were re-incubated in AChE solution for another 2 hours and then placed in Tris–HCl buffer (0.15 mol L^{-1}, pH = 7.4) for 48 hours to remove the unreacted enzyme (Fig. 2f). The obtained AChE-functionalized 2D-PCs were stored in Tris–HCl buffer (0.15 mol L^{-1}, pH = 7.4) at 4 °C.

Determination of AChE activity

For the detection of AChE activity on the 2D-PC hydrogel, 1 × 10^{-3} to 6 × 10^{-3} mol L^{-1} ATChI solutions were prepared in 1.8 × 10^{-4} mol L^{-1} DTNB solution (Tris–HCl buffer, 0.15 mol L^{-1}, pH = 8.0). The AChE-functionalized 2D-PC was then immersed in 1 × 10^{-3} mol L^{-1} to 6 × 10^{-3} mol L^{-1} ATChI solutions at 37 °C under monitoring of UV absorbance at 412 nm for 4 min. In addition, L-cysteine hydrochloride was used as the substitute for thiocholine to acquire the calibration curve.

To determine the amounts of AChE on the 2D-PC hydrogel, 0.025 g of G-250 was added into the mixture of 12.5 mL of ethanol (95 wt%) and 25 mL of phosphoric acid (85 wt%). After being thoroughly stirred, the solution was placed at room temperature overnight and then diluted to 0.1 mg mL^{-1} with water. Subsequently, 2 mL of the G-250 solution (0.1 mg mL^{-1}) was mixed with 50 μL of the AChE solution before and after modification and then, the UV absorbance at 595 nm was recorded.

Detection of Dipterex

The Debye ring and the structural color of the 2D-PC was monitored by a laser pointer with a wavelength of 405 nm and a camera, respectively. Dipterex aqueous solutions from 10^{-4} mol L^{-1} to 10^{-14} mol L^{-1} were prepared using ultrapure water, each of which was adjusted to pH = 7.0 with 0.1 mol L^{-1} NaOH. The AChE-functionalized 2D-PCs were pre-equilibrated in water (pH = 7.0) for 1 hour prior to be immersed in 50 mL Dipterex solutions; the diameter of the Debye ring and the structural color were simultaneously recorded after they were unchangeable. Besides, a control experiment was performed using unfunctionalized 2D-PCs while keeping the other conditions the same.

Results and discussion

Characterization of the 2D-PC

The SEM images were taken by a HITACHI S4800 field emission scanning electron microscope (Tokyo, Japan). As illustrated in Fig. 3a and b, the PS particles (~600 nm) were uniform enough to self-assemble into a 2D-PC array with a periodically close-packed hexagonal monolayer, which was removed from the water surface onto a glass slide. The 2D-PC hydrogel was equilibrated in water and then dried in air before SEM imaging. Fig. 3c and d show that the infiltration of the hydrogel did not destroy the periodicity of 2D-PC, but the close-packed structure turned into a non-close-packed arrangement, which was triggered by the swelling behavior of the hydrogel in water.

Characterization of AChE-functionalized 2D-PC

2D-PC could diffract light and form a Debye diffraction ring on the other side of the sample through a homemade detection

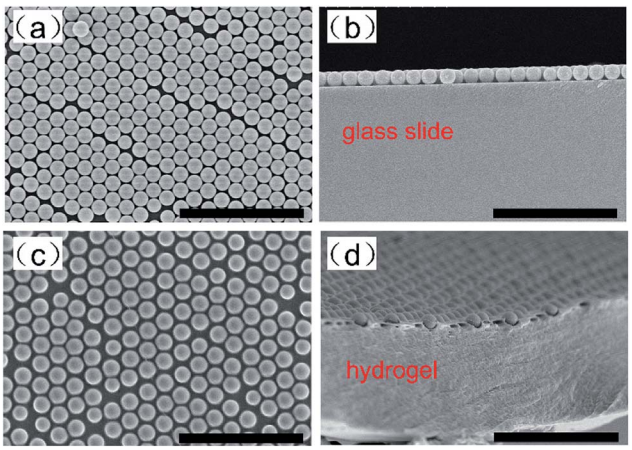

Fig. 3 Top-view (a) and side-view (b) SEM images of the 2D-PC array on a glass slide; top-view (c) and cross-view (d) SEM images of the 2D-PC hydrogel without a substrate; the scale bar is 5 μm.

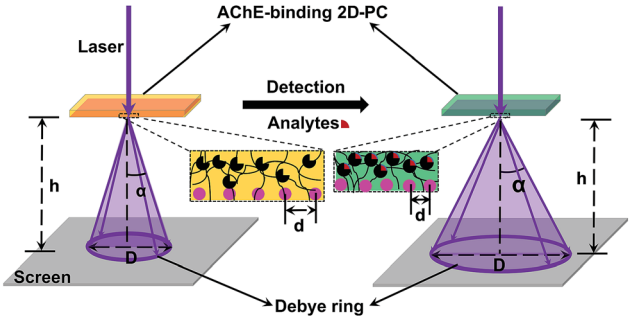

Fig. 4 Diagram of the homemade Debye ring detection device with the change in lattice spacing (d) and diameter of the Debye ring (D) through the process of detection.

device (Fig. 4). Due to the periodicity of the arrangement, the diffraction was in accordance with eqn (1):[28]

$$\sin \alpha = 2\lambda \Big/ \sqrt{3}d \quad (1)$$

here, λ is the wavelength of the monochromatic source (~405 nm), α is the Debye diffraction angle and d is the lattice spacing of 2D-PC, which can be utilized to characterize the order in 2D-PC. Also, as illustrated in Fig. 4, the Debye ring diffraction angle (α), the distance between the screen and sample (h) and the diameter of the Debey ring (D) have certain geometrical relationships, which consequently meet the following equation:

$$\alpha = \text{arc tan } D/2h \quad (2)$$

To verify whether there were carboxyl groups in the 2D-PC hydrogel, the response of the 2D-PC hydrogel to pH 3–12 (0.1 mol L^{-1} phosphate buffer) was investigated prior to immobilization of AChE. As illustrated in Fig. 5a, the lattice spacing of the 2D-PC hydrogel tended to increase with the increasing pH, especially from pH = 4 to 5, which corresponded to the dissociation constant ($pK_a = 4.25$) of the AA monomer.[31] The control experiment of the 2D-PC hydrogel without AA was carried out and no clear change was observed. This suggested that the obtained 2D-PC hydrogel indeed contained carboxyl groups for further modification.

The enzyme activity can be employed to characterize the amounts of active AChE having active sites to irreversibly react with organophosphate. Also, the enzyme activity of AChE-functionalized 2D-PC was determined by a modified Ellman's method.[32] Under the catalysis of AChE, ATChI was converted to thiocholine, which further reacted with DTNB at a stoichiometric ratio of 1 : 1 to form a yellow product. The linear hydrolysis rate of ATChI was calculated using a UV spectrophotometer for the first 4 min for each concentration. Because of the instability of thiocholine, L-cysteine hydrochloride, which also contained a thiol group, was used as a substitute to obtain the standard curve (Fig. S1†). The Michaelis–Menten curve of the AChE-functionalized 2D-PC (Fig. 5b) showed that the maximum hydrolysis rate V_{max} was 0.081×10^{-6} mol min^{-1} cm^{-2}, which indicated that AChE was determined as 0.081 units

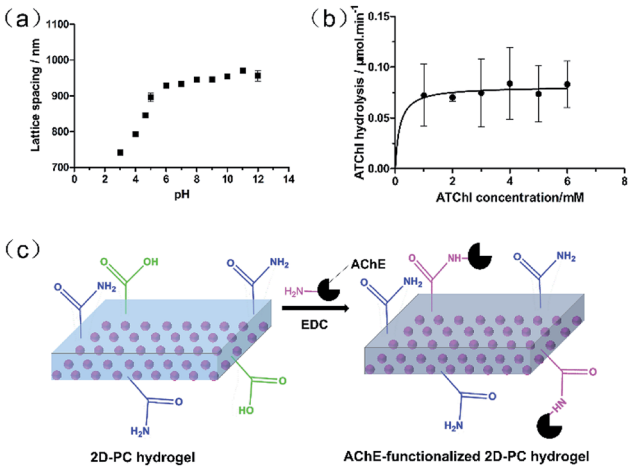

Fig. 5 (a) The lattice spacing of the 2D-PC hydrogel response to different pH values before modification with AChE; (b) Michaelis–Menten curve of the AChE-functionalized 2D-PC; (c) the binding mechanism of AChE and the 2D-PC hydrogel.

in every square centimeter of the 2D-PC hydrogel, and at least 1.4×10^{-12} mol of active AChE was attached to the sensor. Also, the amount of AChE on the 2D-PC hydrogel was 0.43 mg cm^{-2} (Table S2†), according to the G-250 method.[33] The calibration curve is depicted in Fig. S2.† In addition, the mechanism of AChE immobilization onto the 2D-PC hydrogel is described in Fig. 5c. The carboxyl groups of the 2D-PC hydrogel reacted with the amino groups of AChE in the presence of the condensing agent EDC.

Detection of Dipterex

The selectivity of AChE-functionalized 2D-PC is shown in Fig. 6a. The lattice spacing of the objects was divided by that of Dipterex and applied as variables. Under the same concentration of 10^{-4} mol L^{-1}, the variables of the organophosphates such as dichlorvos, malathion, methidathion, acephate and glufosinate-ammonium were 47.7%, 104%, 104%, 82.8% and

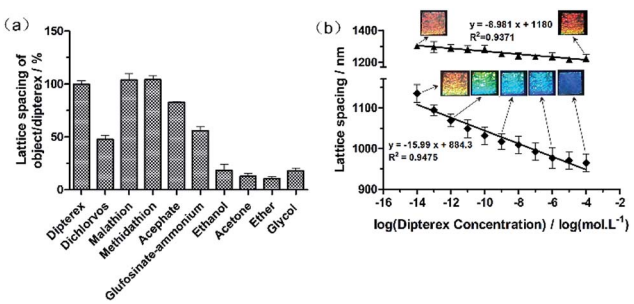

Fig. 6 (a) The selectivity of AChE-functionalized 2D-PC to organophosphates and common organic compounds with the concentration of 10^{-4} mol L^{-1}; (b) AChE-functionalized 2D-PC (◆) and unfunctionalized 2D-PC (▲) for Dipterex detection. The photographs were taken with the camera along the normal while having the light source below at an angle of 45° to the normal of the 2D-PC sensor. Each data point is an average of three measurements.

56.3%, respectively. This indicated that AChE-functionalized 2D-PCs exhibited a good response to Dipterex and its analogs, *i.e.*, malathion and methidathion. However, compared with the other two organophosphates, Dipterex had better water solubility (Fig. S3†), which was similar to those of G-series nerve agents. Thus, Dipterex was finally determined as the substitute for nerve agents to proceed with the next experiment. Meanwhile, a control experiment was used to investigate the response of AChE-functionalized 2D-PC to different types of organic compounds, which had similar water-soluble properties to Dipterex. As illustrated in Fig. 6a, the response signals of the sensor to these organic compounds were much lower than those to Dipterex and the other organophosphates, which indicated that AChE-functionalized 2D-PC exhibited better selectivity to organophosphates. Also, the slight responses were caused by the increase in ionic strength due to the addition of these organic compounds.

The structural color and the lattice spacing of AChE-functionalized 2D-PC and those of unfunctionalized 2D-PC in response to Dipterex are shown in Fig. 6b. When Dipterex concentration increased from 10^{-14} mol L^{-1} to 10^{-4} mol L^{-1}, the lattice spacing of AChE-functionalized 2D-PC decreased from 1135 nm to 965 nm accompanied by structural color change from yellow to blue. Also, linearity of 0.948 was observed between the lattice spacing of 2D-PC and the logarithm of Dipterex concentration. In contrast, the lattice spacing of the unfunctionalized 2D-PC hydrogel varied from 1302 nm to 1226 nm within the same concentration range, and no clear change in the structural color was observed. According to the system we used to observe the structural color, the 2D Bragg diffraction equation (eqn S4 in ESI†) was obtained to calculate the diffracted wavelength (for the detailed derivation process, please see Section 6.1 in ESI†). As shown in Fig. S4,† we could see that when the Dipterex concentration was increased from 10^{-14} mol L^{-1} to 10^{-4} mol L^{-1}, the wavelength of AChE-functionalized 2D-PC changed from 695 nm to 591 nm in the visible region. At the same condition, the wavelength of the unfunctionalized 2D-PC varied from 797 nm to 750 nm. According to the exhibited structural color, the calculated diffracted wavelength was relatively larger than the experimentally obtained diffracted wavelength. One of the possible reasons is that the calculated wavelength represents the diffracted wavelength in vacuum,[34] which is larger than the wavelength in another medium. Even though the structural color detection has big advantage of direct naked-eye observation, this detection was angle-dependent, which made it inconvenient to ensure appropriate illumination angle and the observation angle and created the possibility to induce errors in field detection. In comparison with visual detection, the Debye ring detection could not only ensure the quantitative detection of Dipterex, but also had high accuracy after the construction of the standard line.

After the introduction of AChE, the decrease in the blue-shift of 2D-PC was almost as twice as that of unfunctionalized 2D-PC during the detection of Dipterex at the same concentration range. Thus, we speculated that the blue-shift of AChE-functionalized 2D-PC corresponded to the synergistic effect of two kinds of effects. One was the increase in ionic strength after the addition of organophosphates as a higher ionic strength can screen the Donnan potential and finally induce the shrinking behaviour of 2D-PC.[31] Also, this was the reason that led to the shrinkage of the unfunctionalized 2D-PC. Another combination came from the specific interaction of AChE with organophosphates.[35,36] As for the AChE-functionalized 2D-PC, the pH (7.0) during the organophosphate detection was relatively higher than the isoelectric point of AChE. Before the attachment of organophosphates, the AChE-functionalized 2D-PC was negatively charged. After the active sites were occupied by organophosphates, the charges on the AChE-functionalized 2D-PC decreased and finally weakened the repulsive interaction in the hydrogel, which also induced decrease in the lattice spacing of 2D-PC and simultaneously blue shifted the structural color, according to the 2D Bragg diffraction equation (eqn S4†). Since all the organophosphates could combine with AChE based on this mechanism, the sensor exhibited responsivity to all of these organophosphates in different degrees according to their affinities to the sensor. Both of these led to the shrinkage of the hydrogel and finally caused a decrease in the lattice spacing and a blue-shift in the structural color, which clearly strengthened the detection signal of the AChE-functionalized 2D-PC to organophosphates.

The limit of detection (LOD) based on 3.3 σ/S (where σ is the standard deviation of the blank and S is the slope of the calibration curve) as required by the International Conference on Harmonisation of Technical Requirements for Registration of Pharmaceuticals for Human Use Q2 (ICH Q2) was equal to 7.7×10^{-15} mol L^{-1} (for the detailed process, please see Part 3 in ESI†). The detection performance of our sensor was compared with that of the other reported novel materials such as graphene and MOF materials, and the results are shown in Table S4.† The comparison data indicated that the detection device of AChE-functionalized 2D-PC sensor was the simplest among these novel materials, and it simultaneously exhibited a broad detection range, a low detection limit and good stability. It was also verified that the 2D-PC sensor was the most desired sensor for the onsite screening of organophosphates.

The comparison of different methods for the detection of nerve agents is shown in Table S4 (ESI†); we found that the sensitivity of our sensor was much better than that of other analytical methods. Moreover, after comparing with former 3D-PC, we inferred that the novel 2D-PC sensor was easy to prepare and could form a simple detection device, which was also a big development on the basis of the former study. The previously prepared AChE-functionalized 3D-PC by our group[27] had already realized the detection of organophosphates, but the sensor required the transformation of amide groups into carboxyl groups before the attachment of AChE because the self-assembly of non-close packed 3D-PC was disturbed by ionic monomers such as AA in the hydrogel. However, in this study, AA was directly added to the hydrogel due to different forces of the assembly process, which remarkably simplified the modification process. In addition, compared with the optical fiber spectrometer used in the 3D-PC detection, the detection device of 2D-PC is clearly cheap and convenient. It is not only cost-

effective, but it makes the sensor practicable for onsite screening. Also, the clear change of the structural color helps realize visual detection, due to which AChE-functionalized 2D-PC is a very promising universal sensor for the detection of different organophosphates. Since 2D-PC aims to detect the existence of widely used organophosphates, the high specificity to various organophosphates is not the most important factor that needs to be considered. The binding of AChE with organophosphates is irreversible, which also determines the single-use and disposable function. However, due to the easy and low-cost production, a test paper-like sensor is possible based on this research. Actually, the AChE-functionalized PC hydrogel would not swell or shrink under high ionic strength.[24] A real sample, such as surface water, contains many complicated compositions that cause high ionic strength. Thus, there are some challenges that need to be overcome to apply this 2D-PC sensor in real samples.

Conclusions

A 2D-PC biosensor functionalized with AChE was developed to visually detect a typical organophosphate Dipterex, and it exhibited good water solubility and optical response. Compared with non-close-packed 3D-PC, 2D-PC not only simplified the modification process due to the direct addition of AA into the hydrogel, but also realized the visual detection by naked eyes and a simple determination through the measurement of the Debye ring. A linearity value with 0.9475 was observed between the lattice spacing of the AChE-functionalized 2D-PC sensor and the logarithm of the Dipterex concentration from 10^{-14} mol L^{-1} to 10^{-4} mol L^{-1} following the structural color variation from yellow to blue. Also, LOD of 7.7×10^{-15} mol L^{-1} was achieved. 2D-PC not only shortened the fabrication procedure, but also provided promising potential for the onsite and fast screening of organophosphates.

Conflicts of interest

There are no conflicts to declare.

Acknowledgements

This work was financially supported by the National Natural Science Foundation of China (No. 21375009, U1530141).

Notes and references

1 R. Gotor, P. Gavina, L. E. Ochando, K. Chulvi, A. Lorente, R. Martinez-Manez and A. M. Costero, *RSC Adv.*, 2014, **4**, 15975–15982.
2 A. Barba-Bon, A. M. Costero, S. Gil, A. Harriman and F. Sancenon, *Chem.–Eur. J.*, 2014, **20**, 6339–6347.
3 S. El Sayed, L. Pascual, A. Agostini, R. Martinez-Manez, F. Sancenon, A. M. Costero, M. Parra and S. Gil, *ChemistryOpen*, 2014, **3**, 142–145.
4 B. Della Ventura, R. Funari, C. Altucci, R. Velotta and IEEE, *presented in part at the 2014 Third Mediterranean Photonics Conference*, 2014.
5 R. Funari, B. Della Ventura, L. Schiavo, R. Esposito, C. Altucci and R. Velotta, *Anal. Chem.*, 2013, **85**, 6392–6397.
6 J. Jiang, L. Ou-Yang, L. Zhu, J. Zou and H. Tang, *Sci. Rep.*, 2014, **4**, 3942–3942.
7 W. Ahn, Y. Qiu and B. M. Reinhard, *J. Mater. Chem. C*, 2013, **1**, 3110–3118.
8 P. Prashant and S. S. Seo, *Int. J. Polym. Anal. Charact.*, 2009, **14**, 481–492.
9 P. Prashant and S. S. Seo, *Int. J. Polym. Anal. Charact.*, 2010, **15**, 98–109.
10 M.-P. N. Bui and S. S. Seo, *Anal. Sci.*, 2014, **30**, 581–587.
11 F. Liu, S. Huang, F. Xue, Y. Wang, Z. Meng and M. Xue, *Biosens. Bioelectron.*, 2012, **32**, 273–277.
12 G. L. Turdean, I. C. Popescu, L. Oniciu and D. R. Thevenot, *J. Enzyme Inhib. Med. Chem.*, 2002, **17**, 107–115.
13 X. Li, Z. Xie, H. Min, Y. Xian and L. Jin, *Electroanalysis*, 2007, **19**, 2551–2557.
14 C. Teller, J. Halamek, J. Zeravik, W. F. M. Stoecklein and F. W. Scheller, *Biosens. Bioelectron.*, 2008, **24**, 111–117.
15 X. Sun and X. Wang, *Biosens. Bioelectron.*, 2010, **25**, 2611–2614.
16 X. Li, Z. Xie, H. Min, C. Li, M. Liu, Y. Xian and L. Jin, *Electroanalysis*, 2006, **18**, 2163–2167.
17 N. Ngoc Hai, D. Thi Giang, H. Van Nong, P. Nam Thang, D. Tran Cao and P. Thu Nga, *Adv. Nat. Sci.: Nanosci. Nanotechnol.*, 2015, **6**, 015015.
18 Z. Li, Y. Wang, Y. Ni and S. Kokot, *Sens. Actuators, B*, 2014, **193**, 205–211.
19 D. N. Kumar, A. Rajeshwari, S. A. Alex, M. Sahu, A. M. Raichur, N. Chandrasekaran and A. Mukherjee, *RSC Adv.*, 2015, **5**, 61998–62006.
20 C. Lai, L. Qin, G. Zeng, Y. Liu, D. Huang, C. Zhang, P. Xu, M. Cheng, X. Qin and M. Wang, *RSC Adv.*, 2016, **6**, 3259–3266.
21 C. Zhang, C. Lai, G. Zeng, D. Huang, L. Tang, C. Yang, Y. Zhou, L. Qin and M. Cheng, *Biosens. Bioelectron.*, 2016, **81**, 61–67.
22 M. Saleem, L. P. Lee and K. H. Lee, *J. Mater. Chem. A*, 2014, **2**, 6802–6808.
23 K. Khaldi, S. Sam, A. C. Gouget-Laemmel, C. H. de Villeneuve, A. Moraillon, F. Ozanam, J. Yang, A. Kermad, N. Ghellai and N. Gabouze, *Langmuir*, 2015, **31**, 8421–8428.
24 J. P. Walker and S. A. Asher, *Anal. Chem.*, 2005, **77**, 1596–1600.
25 J. P. Walker, K. W. Kimble and S. A. Asher, *Anal. Bioanal. Chem.*, 2007, **389**, 2115–2124.
26 C. Fenzl, C. Genslein, A. Zoepfl, A. J. Baeumner and T. Hirsch, *J. Mater. Chem. A*, 2015, **3**, 2089–2095.
27 C. X. Yan, F. L. Qi, S. G. Li, J. Y. Xu, C. Liu, Z. H. Meng, L. L. Qiu, M. Xue, W. Lu and Z. Q. Yan, *Talanta*, 2016, **159**, 412–417.
28 F. Xue, S. A. Asher, Z. Meng, F. Wang, W. Lu, M. Xue and F. Qi, *RSC Adv.*, 2015, **5**, 18939–18944.

29 Z. Q. Yan, M. Xue, Q. He, W. Lu, Z. H. Meng, D. Yan, L. L. Qiu, L. J. Zhou and Y. J. Yu, *Anal. Bioanal. Chem.*, 2016, **408**, 8317–8323.
30 C. E. Reese and S. A. Asher, *J. Colloid Interface Sci.*, 2002, **248**, 41–46.
31 F. Xue, Z. Meng, F. Qi, M. Xue, F. Wang, W. Chen and Z. Yan, *Analyst*, 2014, **139**, 6192–6196.
32 G. L. Ellman, K. D. Courtney, V. Andres Jr and R. M. Feather-Stone, *Biochem. Pharmacol.*, 1961, **7**, 88–95.
33 V. S. Gasparov and V. G. Degtyar, *Biochemistry*, 1994, **59**, 563–572.
34 J. T. Zhang, L. Wang, J. Luo, A. Tikhonov, N. Kornienko and S. A. Asher, *J. Am. Chem. Soc.*, 2011, **133**, 9152–9155.
35 C. B. Millard, G. Kryger, A. Ordentlich, H. M. Greenblatt, M. Harel, M. L. Raves, Y. Segall, D. Barak, A. Shafferman, I. Silman and J. L. Sussman, *Biochemistry*, 1999, **38**, 7032–7039.
36 J. P. Walker and S. A. Asher, *Anal. Chem.*, 2005, **77**, 1596–1600.